Journal of Industrial and Engineering Chemistry 18 (2012) 898–903

Contents lists available at SciVerse ScienceDirect

Journal of Industrial and Engineering Chemistry

journal homepage: www.elsevier.com/locate/jiec

Preparation of gadolinia doped ceria via metal complex decomposition method: Its application as catalyst for the steam reforming of ethane

Chatchai Veranitisagul [a], Nattamon Koonsaeng [b], Navadol Laosiripojana [c,*], Apirat Laobuthee [d,**]

[a] Department of Materials and Metallurgical Engineering, Faculty of Engineering, Rajamangala University of Technology Thanyaburi, Pathumthani 12110, Thailand
[b] Department of Chemistry, Faculty of Science, Kasetsart University, Bangkok 10900, Thailand
[c] The Joint Graduate School of Energy and Environment, CHE Center for Energy Technology and Environment, King Mongkut's University of Technology Thonburi, Bangkok 10140, Thailand
[d] Department of Materials Engineering, Faculty of Engineering, Kasetsart University, Bangkok 10900, Thailand

ARTICLE INFO

Article history:
Received 28 April 2011
Accepted 14 July 2011
Available online 3 February 2012

Keywords:
Gadolinia doped ceria
Metal complex decomposition
Reforming
Ethane

ABSTRACT

The ceria (CeO_2) and gadolinia doped ceria (GDC; $Ce_{1-x}Gd_xO_{2-\delta}$ with $x = 0.10, 0.15$, and 0.20) catalysts were successfully prepared via metal complex decomposition method at 900 °C for 2 h. The synthesized CeO_2 and GDC were found to have useful activity to convert ethane to syngas via the steam reforming reaction at the temperature range of 800–900 °C. The catalytic activity was improved with increasing Gd doping amount from 0 to 0.1 and 0.15; nevertheless, at higher Gd doping content (0.2), the improvement becomes less pronounced. Among all catalysts, $Ce_{0.85}Gd_{0.15}O_{2-\delta}$ showed the best steam reforming activity; furthermore, the amount of carbon formation over this catalyst was relatively low. These enhancements are mainly due to the high specific surface area and the good oxygen storage capacity (OSC) of the material. During the steam reforming process, the gas–solid reactions between the gaseous components presented in the system (C_2H_6, C_2H_4, and CH_4) and the lattice oxygen (O_x) on the surface CeO_2 or GDC occurs. The reactions of hydrocarbons adsorbed on the surface with O_x ($C_nH_m + O_x \rightarrow nCO + m/2(H_2) + O_{x-n}$) can prevent the formation of carbon species from hydrocarbons decomposition reaction ($C_nH_m \Leftrightarrow nC + m/2H_2$). Moreover, the formation of carbon via Boudouard reaction ($2CO \Leftrightarrow CO_2 + C$) is also reduced by the gas–solid reaction of CO with the lattice oxygen ($CO + O_x \Leftrightarrow CO_2 + O_{x-1}$).

1. Introduction

Solid oxide fuel cell (SOFC) is known as a promising energy conversion device that generates electricity from the electrochemical reaction between hydrogen-rich gas (or syngas) and oxygen [1–3]. Currently, one of the most interesting fuels for SOFC is natural gas consisting mainly of methane. Nevertheless, natural gas also contains significant amounts of higher hydrocarbons mainly ethane (C_2H_6). It is well established that when natural gas is reformed without the primary treatment, the carbon formation can be easily formed on the catalyst surface due to the decomposition of these hydrocarbons at high temperature. SOFC fueled by natural gas therefore requires a small external pre-reformer unit, where the high hydrocarbon components are reformed readily before introducing to the main part of the system [4]. The pre-reforming unit is normally operated at relatively lower temperature, 300–500 °C, in which the carbon formation is thermodynamically unfavored. However, the disadvantage of this installation is the requirement of the heat supplied into this unit, which can reduce the fuel cell efficiency [5]. The approach to this problem in this work is to develop an alternative catalyst that enables higher hydrocarbon conversion with low degree of carbon deposition at SOFC temperature, 800–900 °C. The successful development of this catalyst would help eliminate the requirement of the external pre-reformer, as these high hydrocarbon elements can be simultaneously reformed together with methane at high temperature.

In this study, C_2H_6 was chosen as the inlet fuels since it is the major high hydrocarbon components presented in natural gas. Cerium oxide (CeO_2 or ceria) based material was chosen as the catalyst since it is widely used for a variety of catalytic reactions involving oxidation of hydrocarbons (e.g. automobile exhaust catalysts). Recently, the use of ceria-based catalysts has shown a rapid increase [6]. A high oxygen mobility [7], high oxygen storage capacity [8–13], strong interaction with the supported metal [14], and the modifiable ability [15] render the ceria-based materials very interesting for catalytic application. In detail, CeO_2 is a mixed ionic electronic material which crystallizes in the fluorite structure

* Corresponding author. Tel.: +66 2 872 9014; fax: +66 2 872 6736.
** Corresponding author. Tel.: +66 2 942 8555; fax: +66 2 955 1811.
E-mail addresses: navadol_l@jgsee.kmutt.ac.th (N. Laosiripojana), fengapl@ku.ac.th (A. Laobuthee).

1226-086X/$ – see front matter © 2012 The Korean Society of Industrial and Engineering Chemistry. Published by Elsevier B.V. All rights reserved.
doi:10.1016/j.jiec.2012.01.047

with a face-centered cubic unit cell with space group *Fm3m*. To reduce the electronic conductivity of ceria, some trivalent cations, such as La_2O_3, Gd_2O_3, and Sm_2O_3, were substituted to obtain the ceria doped solid solutions [16–18]. Nowadays, the gadolinia (Gd) doped ceria (GDC) exhibiting superior ionic conductivity has been applied not only as an electrolyte or an anode in SOFC, but also as catalysts or supporting catalysts in the reforming process [16–19]. Up to the present time, although various methods to prepare ceria and doped ceria for distinct applications were reported, a technique exhibiting several advantages over traditional methods continues under development [20–26]. In this present work, ceria and GDC were, therefore, prepared via the metal complex decomposition method, which exhibits many benefits in terms of a simple and effective method, low processing temperatures, and the homogeneity and purity of products. Then, the catalytic activities toward the steam reforming of C_2H_6 of these synthesized materials were investigated.

2. Experimental

2.1. Materials

Cerium(III) chloride hepta-hydrate ($CeCl_3{\cdot}7H_2O$) was purchased from Acros Organics. Gadolinium(III) chloride hexahydrate ($GdCl_3{\cdot}6H_2O$) was obtained from Sigma. Triethanolamine (TEA, $N(CH_2CH_2OH)_3$) and propan-1-ol ($CH_3CH_2CH_2OH$) were purchased from Carlo Erba.

2.2. Instrumental

The decomposition aspect and weight loss of all the cerium complexes were studied by thermal analysis which carried out with a TGA/DSC analyzer (Model TGA/DSC1, Mettler Toledo). Samples were loaded in an alumina crucible and heated at the heating rate of 10 °C min^{-1} under the air. The weight loss and DSC curves were recorded over the temperature range of 50–1500 °C.

The calcined powders were studied by X-ray diffraction (XRD) using a Bruker D8-Advance X-ray diffractometer with CuK_α radiation. Diffraction patterns were recorded over a range of 2θ angles from 20 to 90° in a step-scanning mode (0.02° steps with a step counting time of 2 s). The crystalline phase was identified from the Joint Committee on Powder Diffraction Standard (JCPDS) file No. 34-0394. The crystallite size, D_{XRD}, of the calcined powders were estimated using the Scherrer equation; $D_{XRD} = 0.9\lambda/\beta \cos\theta$. The λ is the wavelength of the X-ray (1.5406 Å), θ is the scattering angle of the main reflection (1 1 1), and β is the corrected peak at full width at full half-maximum (FWHM) intensity.

Specific surface area (S_{BET}) measurements were carried out using Brunauer–Emmett–Teller (BET) analysis by nitrogen adsorption isotherms at 77 K using a Micromeritics ASAP 2020 surface analyzer and a value of 0.162 nm^2 for the cross section of the nitrogen molecule. Samples were degassed at 350 °C under high vacuum for 20 h before measurement. The S_{BET} were translated into the average particle size (D_{BET}) according to the formula; $D_{BET} = 6000/(d_{th} \times S_{BET})$. The D_{BET} is average particle size (nm), S_{BET} is specific surface area (m^2/g), and d_{th} is the theoretical density of the solid solution oxide (7.211 g/cm^3). The degree of oxygen storage capacity (OSC) was determined by the Temperature Programmed Reduction (TPR) study, which is performed by heating the catalysts up to 900 °C in 5% H_2 in helium. The amount of hydrogen uptake, which correlates to the amount of oxygen store, was then measured.

The powder morphology was observed by scanning electron microscope (SEM, XL30 series, Phillips) operating at an acceleration voltage of 15 kV and 10,000× magnification to identify the powder structures. Samples were mounted on alumina stubs using carbon tape and then sputter coated with Au to avoid particle charging.

2.3. Preparation of $Ce_{1-x}Gd_xO_{2-\delta}$ powders from metal complexes

The complexes of $Ce_{1-x}Gd_xO_{2-\delta}$ ($x = 0$, 0.10, 0.15, and 0.20) were prepared via metal complex decomposition method. The stoichiometric ratios of $CeCl_3{\cdot}7H_2O$ and $GdCl_3{\cdot}6H_2O$ were mixed in propan-1-ol. Triethanolamine (TEA) was then added to the chloride salt solution in the molar ratio of TEA to metal chloride as 1:1. The mixtures were then heated for 3 h to complete the reaction. After removing the solvent, the white powder of cerium complexes was obtained. The decomposition aspect and weight loss of the complexes were studied by TGA/DSC analyzer.

To obtain the $Ce_{1-x}Gd_xO_{2-\delta}$ ceramic powders for catalytic activity study, all of the metal complexes were calcined in an alumina crucible at 900 °C for 2 h in air. The calcined powders were studied by XRD, BET, TPR and SEM.

2.4. Study on catalytic activity of $Ce_{1-x}Gd_xO_{2-\delta}$ powders for ethane steam reforming

An experimental reactor system was constructed from which the feed gases including the components of interest (ethane and steam from the evaporator) and the carrier gas (helium) were introduced to the reaction section, in which an 10-mm diameter quartz reactor was mounted vertically inside a furnace. The catalyst was loaded in the quartz reactor, which was packed with a small amount of quartz wool to prevent the catalyst from moving. The weight of catalyst loading was 50 mg, while the total gas flow was 100 cm^3 min^{-1}. A Type-K thermocouple was placed into the annular space between the reactor and the furnace. This thermocouple was mounted on the tubular reactor in close contact with the catalyst bed to minimize the temperature difference between the catalyst bed and the thermocouple. Another Type-K thermocouple was inserted in the middle of the quartz tube in order to re-check the possible temperature gradient.

During the reactions, the exit gas mixture was transferred via trace-heated lines to the analysis section, which consists of a Porapak Q column Shimadzu 14B gas chromatograph (GC) and a mass spectrometer (MS). The gas chromatography was applied in order to investigate the steady state condition experiments, whereas the mass spectrometer in which the sampling of the exit gas was done by a quartz capillary and differential pumping was used for the transient and carbon formation experiments. In order to study the formation of carbon species on catalyst surface, Temperature Programmed Oxidation (TPO) was applied by introducing 10% oxygen in helium into the system, after purged with helium. The operating temperature increased from room temperature to 1000 °C by the rate of 10 °C min^{-1}. The amount of carbon formations on the surface of catalysts were determined by measuring the CO and CO_2 yields from the TPO results (using Microcal Origin Software). In addition to the TPO method, the amount of carbon deposition was confirmed by the calculation of carbon balance closure in the system. The amount of carbon deposited on the surface of catalyst during the reaction would theoretically be equal to the difference between the inlet carbon containing components (C_2H_6) and the outlet carbon containing components (C_2H_6, CO, CO_2, CH_4, and C_2H_4). The amount of carbon deposited per gram of catalyst is given by the following equation:

$$C_{deposition} = \frac{mole_{carbon(in)} - mole_{carbon(out)}}{m_{catalyst}} \quad (1)$$

The steam reforming reactivity was defined in terms of the conversions and selectivities. Ethane conversion denoted as

X_{Ethane}, and the products selectivity (hydrogen, carbon monoxide, carbon dioxide, methane, and ethylene), denoted as $S_{product}$, are calculated according to Eqs. (2)–(7):

$$X_{Ethane} = \frac{100(\%Ethane_{in} - \%Ethane_{out})}{\%Ethane_{in}} \quad (2)$$

$$S_{H_2} = \frac{100(\%H_2)}{3(\%Ethane_{in} - \%Ethane_{out}) + (\%H_2O_{in} - \%H_2O_{out})} \quad (3)$$

$$S_{CO} = \frac{100(\%CO)}{2(\%Ethane_{in} - \%Ethane_{out})} \quad (4)$$

$$S_{CO_2} = \frac{100(\%CO_2)}{2(\%Ethane_{in} - \%Ethane_{out})} \quad (5)$$

$$S_{CH_4} = \frac{100(\%CH_4)}{2(\%Ethane_{in} - \%Ethane_{out})} \quad (6)$$

$$S_{C_2H_4} = \frac{100(\%C_2H_4)}{(\%Ethane_{in} - \%Ethane_{out})} \quad (7)$$

3. Results and discussion

3.1. Preparation of $Ce_{1-x}Gd_xO_{2-\delta}$ powders from metal complexes

The complexes of $Ce_{1-x}Gd_xO_{2-\delta}$ ($x = 0$, 0.10, 0.15 and 0.20) synthesized from the reaction of $CeCl_3$, $GdCl_3$, and TEA in propan-1-ol were obtained as the homogeneous milky solution after completing the reaction and then changed to the white powders after removing the solvent. All the complexes were converted to ceramic powders by calcination process. Considering the TGA/DSC thermograms of the cerium complexes (Fig. 1(a)) and 10% Gd-doped cerium complex (Fig. 1(b)), the results illustrated that the thermal weight loss characteristic of doped cerium complexes is similar to that of the pure cerium complex. From the TGA/DSC thermograms, it was found that there are three regions of weight loss. The first weight loss occurring before 160 °C resulted from the water evaporation and the removal of organic solvent. The second weight loss happened in temperature ranging from 265 to 484 °C; a large weight loss in TGA curve and a strong exothermic peak in DSC curve at 337 °C involved the decomposition of the organic ligands and generated the char product. The last gradually weight loss occurred at 485–600 °C due to the decomposition of organic and/or carbon-residue. After 600 °C, the TGA thermograms of the complexes showed no weight loss suggesting the temperature for calcining complexes into ceramic powders might be started at 600 °C. In addition, the TGA/DSC thermograms of undoped and Gd-doped cerium complexes exhibit quite similar ceramic yields of CeO_2, and $Ce_{1-x}Gd_xO_{2-\delta}$ around 38–40 wt.%.

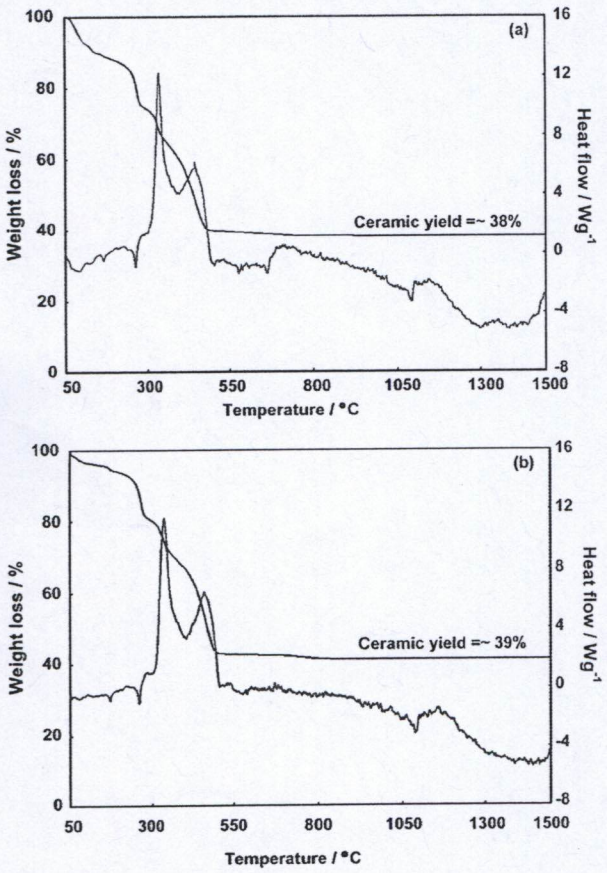

Fig. 1. TGA/DSC thermograms of (a) undoped cerium complex and (b) 10% Gd-doped cerium complex.

To obtain the $Ce_{1-x}Gd_xO_{2-\delta}$ powders for the ethane steam reforming application, all complexes were calcined at 900 °C for 2 h in air. After completing calcination, the light yellowish colored powders of CeO_2, and $Ce_{1-x}Gd_xO_{2-\delta}$ ceramic powders were obtained. The X-ray diffraction patterns of $Ce_{1-x}Gd_xO_{2-\delta}$ powders (Fig. 2) indicated that all compositions of $Ce_{1-x}Gd_xO_{2-\delta}$ are the single phase with a cubic fluorite structure (space group *Fm3m*). All the diffraction patterns are identical to that of the original substance of pure CeO_2 (JCPDS No. 34-0394). This implied the substitution of Gd ions in place of cerium ion lattice site in ceria structure; consequently, no phase change was observed in the CeO_2 crystal defect. However, it was found that the crystallinity of powders decrease with the increasing amount of dopants.

The crystallite size (D_{XRD}), specific surface area (S_{BET}), and average particle size (D_{BET}) of $Ce_{1-x}Gd_xO_{2-\delta}$ powders at 900 °C for 2 h in air are shown in Table 1. It was found that the crystallite sizes of all the powders as calculated from Scherrer equation are less than 100 nm, furthermore, the specific surface area of the materials increases with increasing Gd content until the Gd content of 0.15 then it slightly drop down, whereas the crystallite size and average particle size oppositely decrease with increasing Gd content (until Gd content of 0.15). From the TPR study, the amount of H_2 uptake (Table 1) correlating to the amount of oxygen store, increases with increasing Gd content until Gd content of 0.15; then the effect becomes less pronounce. Nevertheless, it was found that the

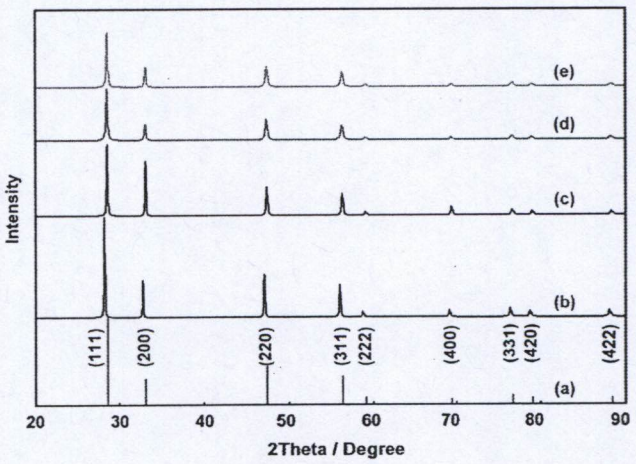

Fig. 2. XRD patterns of (a) reference CeO_2 No. 34-0394 (cubic fluorite structure) and $Ce_{1-x}Gd_xO_{2-\delta}$ powders; (b) $x = 0$, (c) $x = 0.10$, (d) $x = 0.15$, and (e) $x = 0.20$, calcined at 900 °C for 2 h in air.

Table 1
The crystallite size (D_{XRD}), specific surface area (S_{BET}), average particle size (D_{BET}) and total H_2 uptake from the TPR study of $Ce_{1-x}Gd_xO_{2-\delta}$ ($x = 0$, 0.10, 0.15, and 0.20) powders calcined at 900 °C for 2 h in air.

x	Calcination temperature (°C)	Crystallite size, D_{XRD} (nm)	Specific surface area S_{BET} (m^2/g)	Average particle size, D_{BET} (nm)	Total H_2 uptake (from TPR) ($\mu mol/g_{cat}$)
0	900	81.66	3.98	209.06	1768
0.10	900	64.39	7.79	106.81	1932
0.15	900	42.06	21.93	37.94	2353
0.20	900	44.54	17.19	48.40	2304

reduction temperature persistently decreases with increasing Gd content (from 720 °C to 705 °C, 694 °C and 680 °C for GDC with Gd content of 0, 0.10, 0.15 and 0.20 respectively). Fig. 3 represents the SEM micrographs of $Ce_{1-x}Gd_xO_{2-\delta}$ ($x = 0$, 0.10, 0.15, and 0.20) powders calcined at 900 °C for 2 h. All the obtained powders were in irregular shape due to the agglomeration.

3.2. Study on catalytic activity of $Ce_{1-x}Gd_xO_{2-\delta}$ powders for ethane steam reforming

Before studying the catalyst performance, homogeneous (non-catalytic) steam reforming of ethane was carried out. Inlet C_2H_6/H_2O in helium with the molar ratio of 0.1/3.0 was introduced to the system, while the temperature increased from room temperature to 900 °C. It was observed that ethane was converted to methane, ethylene, and hydrogen at the temperature above 700 °C. The significant amount of carbons was also detected in the blank reactor after exposure C_2H_6/H_2O in helium for 10 h. These components were formed via the decomposition of ethane and propane as shown in Eqs. (8)–(10) [27].

$$C_2H_6 \rightarrow C_2H_4 + H_2 \quad (8)$$

$$C_2H_4 \Leftrightarrow 2H_2 + 2C \quad (9)$$

$$C + 2H_2 \rightarrow CH_4 \quad (10)$$

There was no change in the steam concentration, and neither carbon monoxide nor carbon dioxide was produced in the system; this indicates that there is no homogenous reforming reaction (between steam and hydrocarbon elements) takes place under the studied conditions. The steam reforming of ethane by CeO_2 and GDC was then studied at 800–900 °C. At these isothermal conditions, C_2H_6/H_2O in helium with different C_2H_6/H_2O molar ratios of 1.0/1.0, 1.0/2.0, and 1.0/3.0 were introduced in order to compare the reforming rates. Hydrogen production yield after operated for 24 h at various temperatures and inlet C_2H_6/H_2O ratio are shown in Figs. 4 and 5. It can be seen that the steam reforming over GDC (with Gd content of 0.15) using inlet C_2H_6/H_2O of 1.0/3.0 at 900 °C shows the best activity.

The influences of operating temperature and the inlet steam to ethane ratio on the product selectivity were also studied. It was observed that the reforming activity of all catalysts slightly decreases during the first 6 h and reaches the steady state rate after 15–18 h. The initial deactivation is mainly related to the carbon deposition, which is proven by the quantitative carbon balance closure (as presented in the next paragraph). As shown in Fig. 6, at steady state, the main products from this reaction over GDC (with Gd content of 0.15) were H_2, CO, CO_2, and CH_4, with small amount of C_2H_4 depending on the operating temperature. Regarding the influence of inlet steam, hydrogen and carbon dioxide selectivity increased with the increase of inlet steam concentration, whereas carbon monoxide selectivity decreased as shown in Fig. 7. These

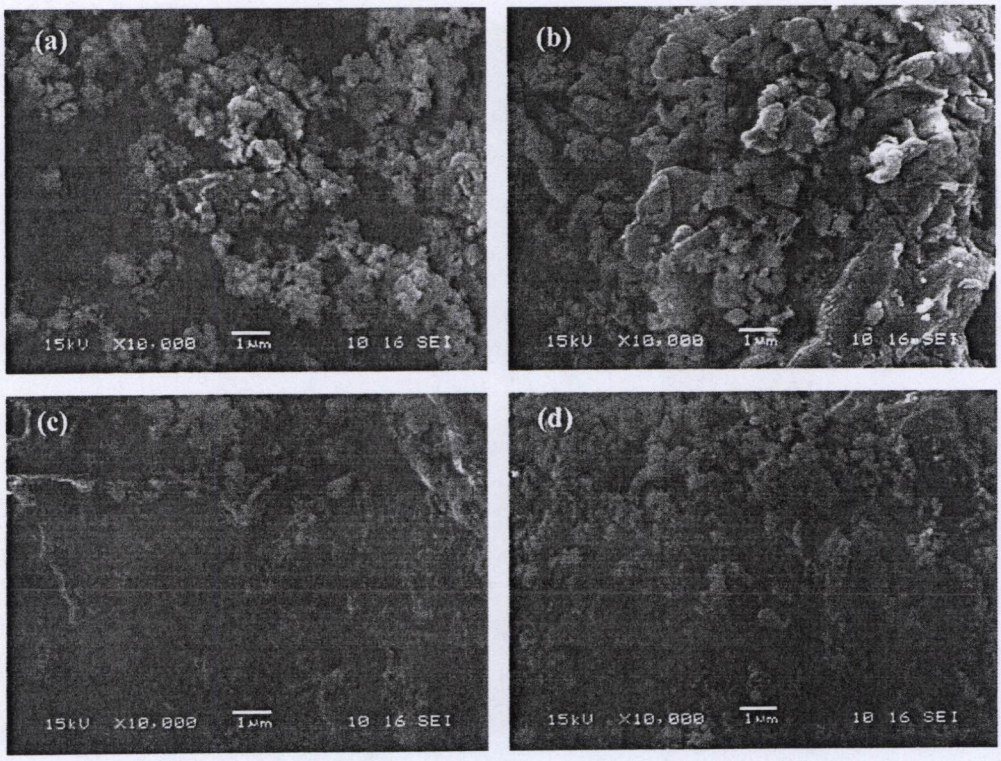

Fig. 3. SEM micrographs of $Ce_{1-x}Gd_xO_{2-\delta}$ powders: (a) $x = 0$, (b) $x = 0.10$, (c) $x = 0.15$, and (d) $x = 0.20$, calcined at 900 °C for 2 h in air.

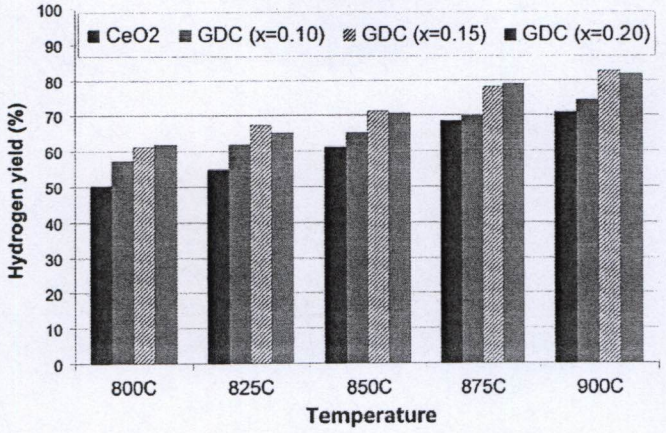

Fig. 4. Effect of temperature on the hydrogen production yield from the steam reforming of ethane over several catalysts (at inlet steam/ethane molar ratio of 1.0/3.0).

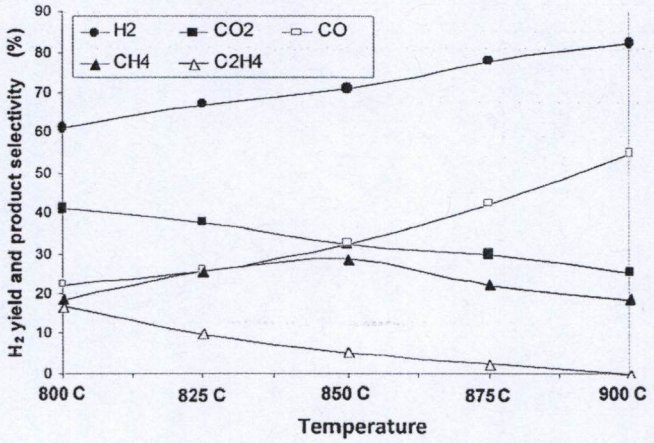

Fig. 6. Effect of temperature on the product selectivity from the steam reforming of ethane over GDC (Gd content of 0.15) at inlet steam/ethane molar ratio of 1.0/3.0.

are mainly due to the influence of water–gas shift reaction ($CO + H_2O \rightarrow CO_2 + H_2$). Moreover, the appearances of methane and ethylene in the system were found to decrease with the increase of steam content, as these components were further reformed to CO, CO_2, and H_2 by the excess steam.

The post-reaction temperature-programmed oxidation (TPO) experiments were carried out after a helium purge by introducing of 10% oxygen in helium in order to determine whether the observed deactivation is from the carbon formation. From the TPO results, the relatively high peaks of carbon dioxide and carbon monoxide were observed for CeO_2, while smaller peaks of both components were detected for GDC. The amount of carbon formations on the surface of these catalysts with different inlet C_2H_6/H_2O ratios were determined by measuring the CO and CO_2 yields from the TPO results; the quantities of carbon deposited over CeO_2 and GDC (with Gd content of 0.1, 0.15 and 0.2) were observed to be approximately 1.76, 1.19, 1.07, and 1.04 mmol g^{-1}. The total amounts of carbon deposited were compared with the calculation of carbon balance in the system. The calculated values were 1.77, 1.15, 1.00 and 1.03 mmol g^{-1}, which are in good agreement with the experimented ones. Theoretically, during the reforming of ethane, the carbon formation could occur due to several reactions, the following reactions are the most probable reactions that could lead to carbon formation:

$$C_2H_6 \Leftrightarrow 3H_2 + 2C \quad (11)$$

$$CH_4 \Leftrightarrow 2H_2 + C \quad (12)$$

$$C_2H_4 \Leftrightarrow 2H_2 + 2C \quad (13)$$

$$2CO \Leftrightarrow CO_2 + C \quad (14)$$

$$CO + H_2 \Leftrightarrow H_2O + C \quad (15)$$

$$CO_2 + 2H_2 \Leftrightarrow 2H_2O + C \quad (16)$$

where *C* is the carbonaceous deposits. The decomposition of hydrocarbons (Eqs. (11)–(13)) and the Boudouard reaction (Eq. (14)) are the major pathways for carbon formation at such a high temperature, whereas Eqs. (15) and (16) are favorable at low temperature [28,29]. Therefore, according to the range of temperature in this study, carbon formation would be formed via the decomposition of hydrocarbons and Boudouard reaction. With the increase of steam to carbon ratio, the equilibrium of water–gas shift reaction moves forward and produces more CO_2 rather than CO. Therefore, high steam feed can avoid carbon deposition via the Boudouard reaction. However, significant amount of carbon could remain detected due to the decomposition of ethane, ethylene, and methane. By using CeO_2 and GDC as the catalyst, these reactions could be inhibited by the gas–solid reactions between hydrocarbons with the lattice oxygen (O_x) at

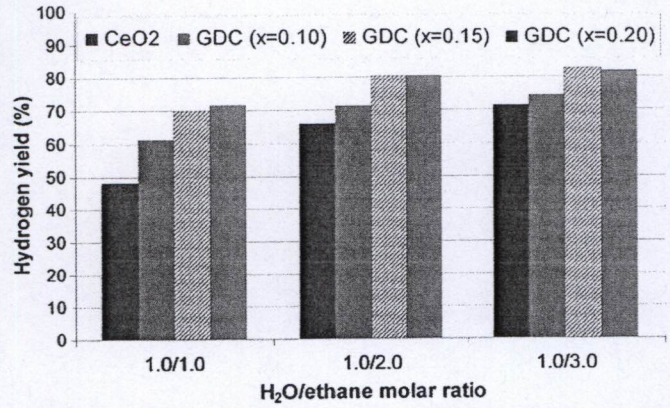

Fig. 5. Effect of inlet steam/ethane molar ratio on the hydrogen production yield from the steam reforming of ethane over several catalysts (at 900 °C).

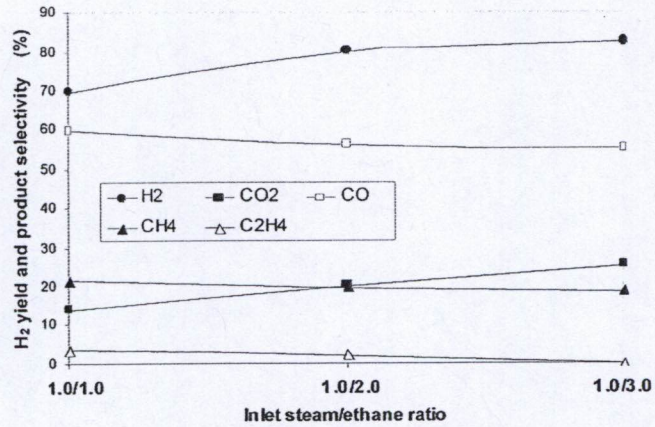

Fig. 7. Effect of inlet steam/ethane molar ratio on the hydrogen production yield from the steam reforming of ethane over GDC (Gd content of 0.15) (at 900 °C).

CeO_2 surface forming hydrogen and carbon dioxide, which are thermodynamically unfavored to form carbon species. The solid-gas mechanism involves the reactions between hydrocarbons (C_2H_6, CH_4, and C_2H_4) and/or an intermediate surface hydrocarbon species with the lattice oxygen (O_x) at CeO_2 surface are presented in Eqs. (17)–(24).

$$C_2H_6 + 2S \Leftrightarrow 2(CH_3{-}S) \quad (17)$$

$$CH_4 + 2S \Leftrightarrow CH_3{-}S + H{-}S \quad (18)$$

$$C_2H_4 + 2S \Leftrightarrow 2(CH_2{-}S) \quad (19)$$

$$CH_3{-}S + S \Leftrightarrow CH_2{-}S + H{-}S \quad (20)$$

$$CH_2{-}S + \Leftrightarrow CH{-}S + H{-}S \quad (21)$$

$$CH{-}S + S \Leftrightarrow C{-}S + H{-}S \quad (22)$$

$$C{-}S + O_x \Leftrightarrow CO + O_{x-1} + S \quad (23)$$

$$2H{-}S \Leftrightarrow H_2 + 2S \quad (24)$$

where S is the catalyst surface site. During the steam reforming, hydrocarbons are adsorbed on either a unique site (S) or the lattice oxygen (O_x), whereas H_2O can react with the reduced site of ceria, O_{x-1}. The steady state reforming rate is mainly due to the continuous supply of the oxygen source by H_2O.

$$H_2O + O_{x-1} \Leftrightarrow O_x + H_2 \quad (25)$$

It should be noted that the solid–gas reaction on the surface of ceria could also reduce the formation of carbon via Boudouard reaction, as carbon monoxide can adsorb and react with the lattice oxygen (O_x) on the surface of ceria forming carbon dioxide ($CO + O_x \Leftrightarrow O_{x-1} + CO_2$), which is less flavored to form carbon species at high temperature. The higher steam reforming activity of GDC (particularly the catalyst with Gd doping content of 0.15 and 0.20) with greater resistance toward carbon deposition compared to CeO_2 is mainly due to its higher OSC according to the TPR results in Table 1, which also closely relates with the material specific surface area. Furthermore, based on the TPR results, the greater reforming activity of GDC (with Gd of 0.20) over GDC (with Gd of 0.15) at low reaction temperature (800 °C) could be due to its lower reduction temperature (680 °C compared to 694 °C), whereas the slightly better reforming activity of GDC (with Gd of 0.15) at 900 °C is due to its higher OSC value.

4. Conclusion

$Ce_{1-x}Gd_xO_{2-\delta}$ ($x = 0$–0.2) solid solutions with the fluorite structure were successfully prepared via metal complex decomposition method at 900 °C for 2 h. GDC (with Gd doping content of 0.15) is a good catalyst for the reforming of ethane at SOFC temperature (800–900 °C). It can provide good hydrogen production yield with high resistance toward the deactivation from carbon formation at high temperature. During reforming process, the gas–solid redox reactions on ceria surface take place and reduce the degree of carbon deposition on catalyst surface from hydrocarbons decomposition and Boudouard reaction.

Acknowledgements

The financial support from Kasetsart University Research and Development Institute (KURDI), Kasetsart University throughout this project is gratefully acknowledged. One author (C. Veranitisagul) also thanks to Thailand Research Fund (Grant No. MRG5480046).

References

[1] W.L. Lundberg, S.E. Veyo, Conceptual design and performance analysis of a 300 MWel LNG-fuelled pressurised SOFC/Gas turbine power plant, in: S.C. Yokohawa, Singhal (Eds.), Proceeding of the 7th International Symposium Solid Oxide Fuel Cells VII, 2001, p. 78.
[2] P. Aguiar, D. Chadwick, L. Kershenbaum, Chem. Eng. Sci. 57 (2002) 1665.
[3] P. Aguiar, N. Lapena-Rey, D. Chadwick, L. Kershenbaum, Chem. Eng. Sci. 56 (2001) 651.
[4] R. Peters, R. Dahl, U. Kluttgen, C. Palm, D. Stolten, J. Power Sources 106 (2002) 238.
[5] N. Laosiripojana, in: 6th European Solid Oxide Fuel Cell Forum, 28 June–2 July, 2004.
[6] A. Trovareli, C. Leitenburg, G. Dolcetti, Chemtech (1997) 32.
[7] P. Fornasiero, G. Balducci, R.D. Monte, J. Kaspar, V. Sergo, G. Gubitosa, A. Ferrero, M. Graziani, J. Catal. 164 (1996) 173.
[8] T. Miki, T. Ogawa, M. Haneda, N. Kakuta, A. Ueno, S. Tateishi, S. Matsuura, M. Sato, J. Phys. Chem. 94 (1990) [339 or 6464–6467].
[9] C. Padeste, N.W. Cant, D.L. Trimm, Catal. Lett. 18 (1993) 305.
[10] S. Kacimi, J. Barbier Jr., R. Taha, D. Duprez, Catal. Lett. 22 (1993) 343.
[11] G.S. Zafiris, R.J. Gorte, J. Catal. 143 (1993) 86.
[12] G.S. Zafiris, R.J. Gorte, J. Catal. 139 (1993) 561.
[13] S. Imamura, M. Shono, N. Okamoto, A. Hamada, S. Ishida, Appl. Catal., A 142 (1996) 279.
[14] L. Fan, K. Fujimoto, J. Catal. 172 (1997) 238.
[15] M. Pijolat, M. Prin, M. Soustelle, O. Touret, P. Nortier, J. Chem. Soc., Faraday Trans. 91 (1995) 3941.
[16] S.P.S. Badwal, K. Foger, Ceram. Int. 22 (1996) 257.
[17] A.B. Stambouli, E. Traversa, Renew. Sust. Energ. Rev. 6 (2002) 433.
[18] G.B. Balazs, R.S. Glass, Solid State Ionics 76 (1995) 155.
[19] E. Ramirez-Cabrera, A. Atkinson, D. Chadwick, Appl. Catal., B 36 (2002) 193.
[20] S. Kuharuangrong, J. Power Sources 171 (2007) 506.
[21] R.S. Torrens, N.M. Sammes, G.A. Tompsett, Solid State Ionics 111 (1998) 9.
[22] A.I.Y. Tok, L.H. Luo, F.Y.C. Boey, Mater. Sci. Eng., A 383 (2004) 229.
[23] Y.P. Fu, S.B. Wen, C.H. Lu, J. Am. Ceram. Soc. 91 (2008) 127.
[24] G. Ruifeng, M. Zongqiang, J. Rare Earth 25 (2007) 364.
[25] S. Dikmen, P. Shuk, M. Greenblatt, H. Gocmez, Solid State Sci. 4 (2002) 585.
[26] R.O. Fuentes, R.T. Baker, Int. J. Hydrogen Energy 33 (2008) 3480.
[27] M.V. Twigg, Catalyst Handbook, second ed., Wolfe Publishing Ltd., London, 1989
[28] Y. Lwin, W.R.W. Daud, A.B. Mohamad, Z. Yaakob, Int. J. Hydrogen Energy 25 (2000) 47.
[29] J.N. Armor, Appl. Catal., A 176 (1999) 159.

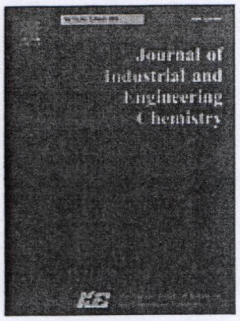

Journal of Industrial and Engineering Chemistry

The official journal of the Korean Society of Industrial and Engineering Chemistry

Publication of the Korean Society of Industrial and Engineering Chemistry

Journal of Industrial and Engineering Chemistry is published bimonthly in English by the Korean Society of Industrial and Engineering Chemistry. *JIEC* brings together multidisciplinary interests in one...

View full aims and scope

Editor-in-Chief: Jyongsik Jang
View full editorial board

Guide for Authors

Submit Your Paper

Order Journal

View Articles

Impact Factor: 2.145

5-Year Impact Factor: 1.955

Imprint: ELSEVIER

ISSN: 1226-086X

Recent Articles

Synthesis, characterization and evaluation of Ni–Mo/Zr–Al2O3 catalyst for hydro-conversion of lignite-based heavy carbon resources
Zhiping Lei | Lian Wu | ...

Development of microwave assisted oxidative desulfurization of petroleum oils: A review
Hui Shang | Haichao Zhang | ...

Sunlight photodecolorization of a mixture of Methyl Orange and Bromocresol Green by CuS incorporated in a clinoptilolite zeolite as a heterogeneous catalyst
Alireza Nezamzadeh-Ejhieh | Neda Moazzeni

VIEW ALL

Most Cited Articles

Polymer micro and nanocomposites: Structure, interactions, properties
Móczó, J. | Pukánszky, B.

Permeable reactive barrier for groundwater remediation
Thiruvenkatachari, R. | Vigneswaran, S. | ...

Review: A chance for Korea to advance algal-biodiesel technology
Um, B.-H. | Kim, Y.-S.

VIEW ALL